Research on Chemical Intermediates
https://doi.org/10.1007/s11164-020-04178-9

Click synthesis of 1,4-disubstituted-1,2,3-triazoles catalyzed by melamine-supported CuO nanoparticles as an efficient recyclable catalyst in water

Mahboobeh Rajabi[1] · **Jalal Albadi**[1] · **Ahmadreza Momeni**[1]

Received: 19 March 2020 / Accepted: 11 May 2020

Abstract

Melamine-supported CuO nanoparticles (M-CuO nanocatalyst) are prepared as a new and efficient recyclable nanocatalyst for the regioselective synthesis of 1,2,3-triazoles in water. This new nanocatalyst was prepared by co-precipitation method and characterized by FT-IR spectral study, TGA, DSC, XRF, ICP-OES, XRD, SEM, EDS and BET analysis. A wide range of 1,4-disubstituted-1,2,3-triazoles were synthesized from reaction of benzyl halides or alkyl halides with phenyl acetylene and sodium azide in high yields. M-CuO nanocatalyst could be reused more than 6 times without considerable loss of its initial activity.

Keywords M-CuO nanocatalyst · Melamine · Click reaction · 1,4-Disubstituted-1,2,3-triazoles

Introduction

Because of their biological and medicinal properties, synthesis of 1,2,3-triazole derivatives has received much attention. 1,2,3-Triazoles are used as industrial dyes, corrosion inhibitors, photostabilizers and photographic materials [1, 2]. The main process for the synthesis of 1,2,3-triazoles is the 1,3-dipolar cycloaddition reaction of azides with alkynes as the model of click reactions [3]. It was found that copper-catalyzed click reaction has proved to be the most suitable synthetic route for the click synthesis of 1,2,3-triazole derivatives [4]. Therefore, catalytic activity of various copper catalysts in the azide–alkyne click reactions has received much attention [5–12]. Among these, copper-supported catalysts have been more attracted attention.

Electronic supplementary material The online version of this article (https://doi.org/10.1007/s11164-020-04178-9) contains supplementary material, which is available to authorized users.

✉ Jalal Albadi
chemalbadi@gmail.com; albadi@sku.ac.ir

[1] Department of Chemistry, Faculty of Science, Shahrekord University, Shahrekord, Iran

Published online: 18 May 2020

Regarding the great importance of the support in these catalysts, various supports have been used for the preparation of copper-supported catalysts [13–25]. The best supports are those which have nitrogen or oxygen binding sites and are chelated with copper catalysts. Nitrogen-based compounds have shown to protect the metal center from oxidation and disproportionation, while enhancing their catalytic activity [26]. Therefore, there is a scope to develop the introduction of a new, simple and efficient support for the preparation of these catalysts.

Moreover, the supported copper nanoparticles exhibit higher activity and selectivity, because of their high surface area, catalyst loading capacity and good dispersion. Thus, the preparation of new, simple and efficient copper-supported nanocatalyst may afford an opportunity to reach new catalytic system with practical high-performance applications. Melamine (2,4,6-triamino-1,3,5-triazine), an stable organic compound, is prepared readily and is commercially available. Due to having nitrogen in its structure and high loading capacity, melamine can be used as a simple and efficient support for the copper nanocatalysts. However, to the best of our knowledge, there is no report which utilizes melamine as a support for the preparation of copper-supported nanocatalyst.

In continuation of our researches on the development of novel nanocatalysts [27–31], herein, we wish to report the preparation, characterization and catalytic study of melamine-supported copper oxide nanoparticles (M-CuO nanocatalyst) as a new, efficient and recyclable nanocatalyst for the regioselective synthesis of 1,4-disubstituted-1,2,3-triazoles in water (Scheme 1).

Experimental

Chemical materials were purchased from Merck chemical companies. Prepared products were characterized by the evaluation of their spectroscopic data (^{1}H NMR, ^{13}CNMR, IR) and physical properties with those reported in the literature. The XRF analysis was done by a Philips Venus 100 minilab instrument. The ICP analysis was performed by a Vista-pro varian instrument. The XRD investigation was performed using an X-ray diffractometer, Cu-Kα monochromatized radiation source and a

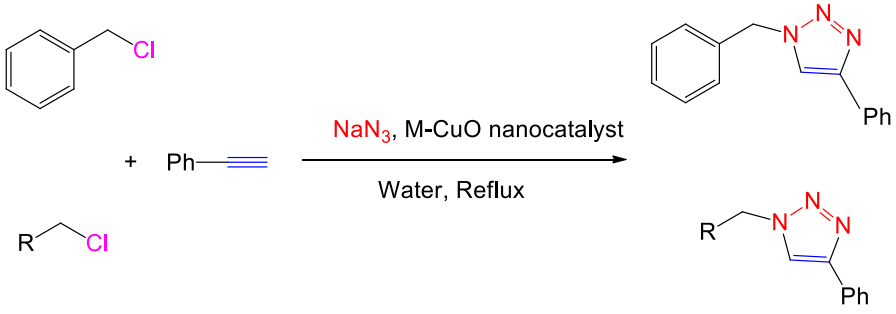

Scheme 1 M-CuO nanocatalyst-catalyzed regioselective synthesis of 1,4-disubstituted-1H-1,2,3-triazoles

nickel filter (PANalytical X'Pert-Pro). Scherrer equation was used to determine the average crystallite size of the sample. The morphology of the nanocatalyst was studied by field emission scanning electron microscopy (FESEM) method by a JEOL JSM-6500F instrument, equipped with an EDS analytical system. The BET surface area was tested by N_2 adsorption–desorption method. The analysis was carried out using an automated gas adsorption analyzer (Tristar 3020, Micromeritics). The sample was purged with nitrogen gas for 3 h at 300 °C by a VacPrep 061 degas system (Micrometrics).

Catalyst preparation

The melamine-supported copper oxide nanoparticles (M-CuO nanocatalyst) were prepared via a co-precipitation process. At first, Na_2CO_3 solution (0.5 M) was added drop-wise into a mixture of Cu $(NO_3)_2{\cdot}3H_2O$ (0.03 M) and melamine (3 g), under vigorous stirring for 24 h at 70 °C. Then, the obtained solid was filtered, washed with deionized water and dried 2 h at 100 °C followed by calcination at 250 °C for 3 h to afford the M-CuO nanocatalyst.

General procedure

A mixture of benzyl halide or alkyl halide (1 mmol), alkyne (1 mmol), sodium azide (1.1 mmol) and M-CuO nanocatalyst (0.04 g) was stirred in water at reflux condition. After reaction completion (monitored by TLC), the reaction mixture was cooled and catalyst was filtered. The recovered catalyst was washed with hot acetone, dried and stored for another following reaction run. Then the filtrate was evaporated to dryness, and the solid residue was recrystallized in ethanol/water (3:1 v/v) to give corresponding pure products.

Results and discussion

Catalyst characterization results

The FESEM images and the EDS results of the melamine and melamine-supported CuO nanoparticles are shown in Fig. 1. The FESEM analysis shows the presence of some nanoparticles of melamine with particle sizes less than 68 nm, remained on the surface of bulk melamine (Fig. 1a). It seems that the CuO nanoparticles, with particle diameters less than 34 nm, distributed on the outer surface of the melamine substrate (Fig. 1b). It is valuable to note that the CuO component could be precipitated as larger particles in final catalyst. However, the presence of nanoparticles in this product is evident. The comparison of the EDS analysis, as shown in Fig. 1c, d, presented the Cu content of about 9.28% w w^{-1} which is in agreement with the results obtained by ICP-OES (9.46% w w^{-1}) and X-ray fluorescence (9.53% w w^{-1}). According to this agreement, one can state that the CuO nanoparticles settled on the surface of the support.

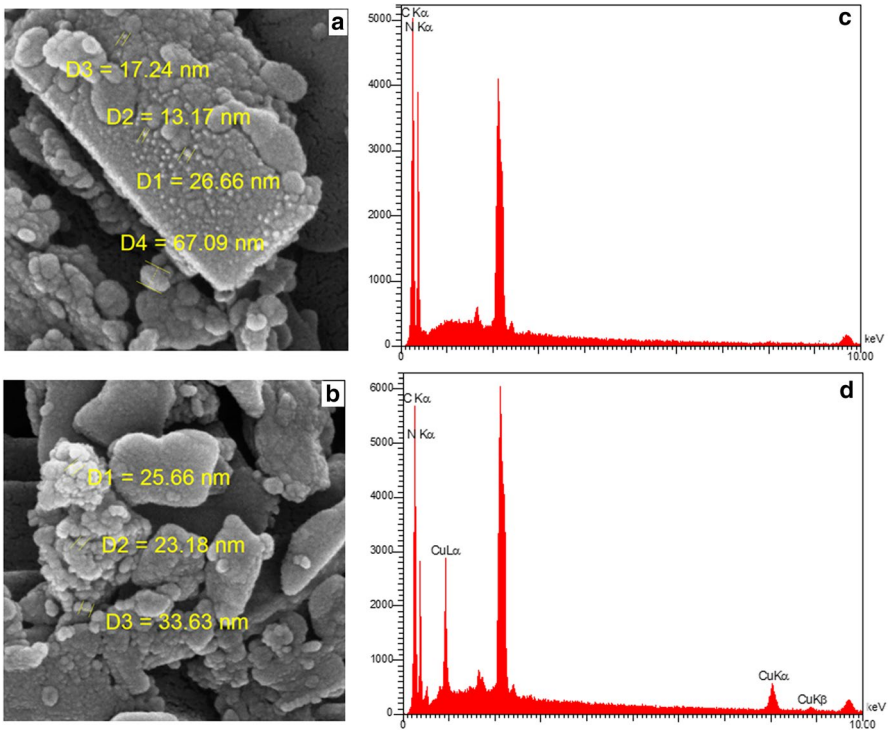

Fig. 1 The FESEM images of melamine (**a**) M-CuO nanocatalyst (**b**), the EDS analysis of melamine (**c**) M-CuO nanocatalyst (**d**)

In order to investigate the thermal stability of the prepared nanocatalyst, and also to identify a temperature range for calcination, the TGA and DSC tests were performed. The obtained TGA and DSC plots are shown in Fig. 2. The first weight loss feature took place after 200 °C is related to desorption and evaporation of H_2O molecules and formation of CuO [32]. The second weight loss feature occurred on the temperature greater than 280 °C is attributed to the NH_3 volatilization and melem ($C_6H_6N_{10}$) formation, and the third weight loss feature is ascribed to the conversion of the $C_6H_6N_{10}$ to the graphitic carbon nitride (g-C_3N_4).

In order to detect the loading of the CuO nanoparticles on the melamine support (M-CuO) or coordinated to it, the X-ray diffraction was conducted. The obtained patterns for the melamine support and M-CuO are shown in Fig. 3a, b, respectively. The indexed prominent peaks centered at $2\theta = 13.1$, $2\theta = 15.2$, $2\theta = 17.9$, $2\theta = 21.8$, $2\theta = 21.9$, $2\theta = 26.2$, $2\theta = 27.1$ and $2\theta = 29.4$ were attributed to the melamine crystalline planes [32–34]. As shown in Fig. 3b, the loading of CuO nanoparticles did not significantly change the XRD pattern corresponding to the melamine support. It is obvious that the peaks centered at about $2\theta = 38.1$, $2\theta = 47.4$ and $2\theta = 36.5$ are attributed to the crystalline planes of 002, 111 and

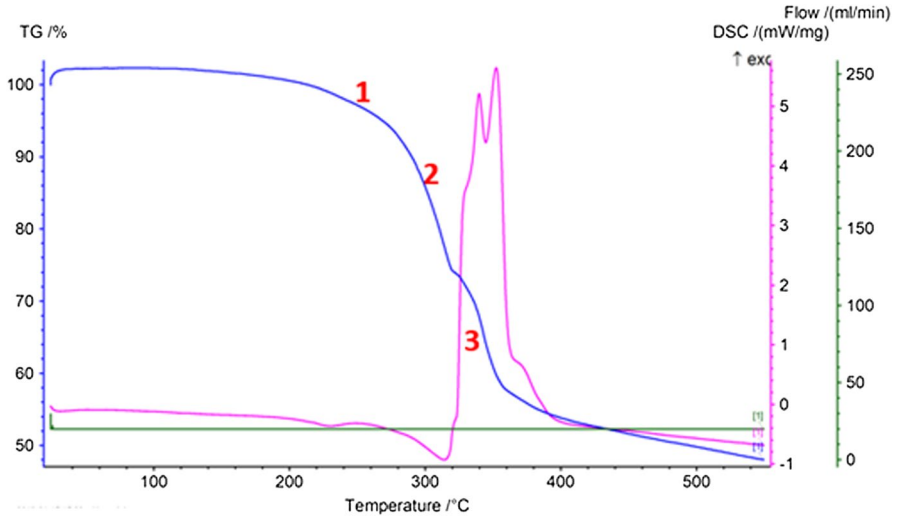

Fig. 2 TGA and DSC of the M-CuO nanocatalyst

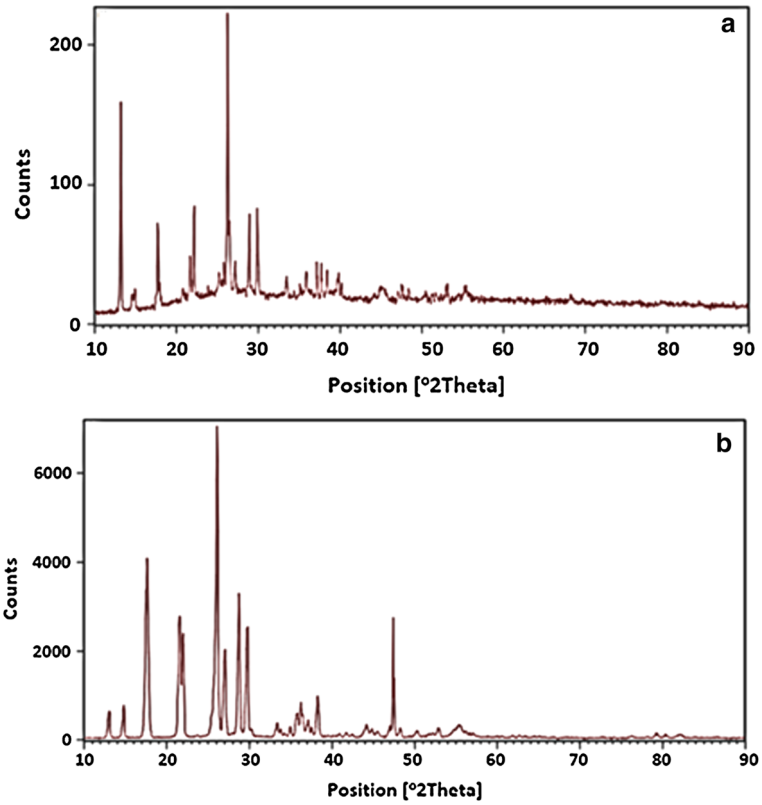

Fig. 3 XRD pattern of melamine (**a**) and M-CuO nanocatalyst (**b**)

202 of nanoparticles of CuO [35]. However, the XRD pattern of the catalyst after incorporating of the CuO, and then calcination, demonstrated that the crystalline properties of the nanocatalyst have been remained.

The N_2 adsorption/desorption isotherm of the melamine support and the nanocatalyst has been recorded and is shown in Fig. 4a. According to the IUPAC classification, the isotherms for both samples are same as the isotherm pattern III. The obtained isotherm demonstrated that the melamine support and M-supported CuO nanocatalyst exhibit a hysteresis loops between $p/p^0 = 0.6–0.97$ and 0.4–0.97, respectively. It can be stated that the incorporation of the CuO and calcination phenomena changed the agglomeration [36], porosity and interface chemistry between N_2 phase and the resulted nanocatalyst, so that the pressure range of the hysteresis loop extended.

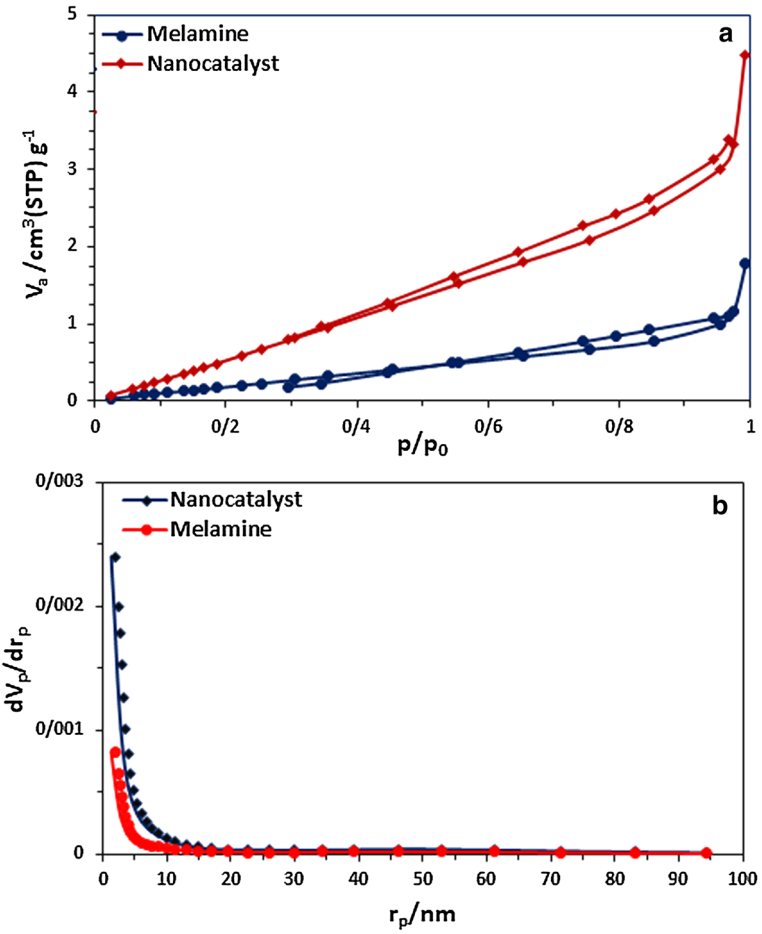

Fig. 4 N_2 adsorption/desorption isotherms (**a**) and pore diameter size distribution (**b**) of the melamine (**a**) and M-CuO nanocatalyst

Table 1 Structural properties of the melamine support and M-CuO nanocatalyst (BET analysis)

Sample	BET surface area ($m^2\ g^{-1}$)	Average pore size (nm)	Pore volume ($cm^3\ g^{-1}$)
Melamine	1.012	10.232	0.0026
M-CuO nanocatalyst	3.247	8.318	0.0067

Table 2 Optimization of the reaction conditions

Entry	Solvent/temperature	Catalyst amount (g)	Time (min)	Yield (%)[a]
1	EtOH/r.t.	–	60	–
2	EtOH/reflux	–	60	–
3	EtOH/r.t.	0.03	60	–
4	EtOH/r.t.	0.05	60	–
5	EtOH/reflux	0.03	60	Trace
6	EtOH/reflux	0.04	60	50
7	EtOH/reflux	0.05	60	50
8	EtOH/reflux	0.1	60	60
9	H_2O/r.t.	–	60	–
10	H_2O/r.t.	0.03	60	–
11	H_2O/r.t.	0.05	60	Trace
12	H_2O/reflux	0.03	30	70
13	H_2O/reflux	0.04	12	92
14	CH_3CN/r.t.	0.04	60	–
15	CH_3CN/reflux	0.04	60	25

[a]Isolated pure products

The obtained BJH graphs shown in Fig. 4b present that most sizes of the pores diameter are less than 10 nm for both support and nanocatalyst. It is obvious that the increase in the BET surface area, total pore volume and decrease in the pore diameter of the nanocatalyst with respect to the melamine support are due to the presence of the CuO nanoparticles on the surface of the support (Table 1). Therefore, the BET data can be a proof to prove the formation of the CuO active catalyst sites on the support.

Catalytic performance

At first, to optimize the reaction conditions, the reaction of benzyl chloride, phenyl acetylene and sodium azide was selected as a model reaction and its manners were studied under various conditions (Table 2).

Several factors such as solvent, temperature and catalyst amount were checked. Various catalyst amounts were studied and it was found that using 0.04 g of M-CuO nanocatalyst gave the best results. Among the various solvents that were

studied, water was better solvent and it was found that the corresponding product was obtained in higher yield and shorter reaction time under reflux condition. Therefore, M-CuO nanocatalyst (0.04 g) in water at reflux conditions was selected to be the most conditions for this reaction. Moreover, the performance of various M-CuO nanocatalysts containing 5, 9.4 and 15 wt.% CuO, on this reaction, were investigated. As given in Table 3, the M-CuO nanocatalyst containing about 9.4 wt.% CuO showed the highest yield of reaction of about 92%, in relatively lower reaction time (12 min).

Using these optimized conditions, the synthesis of 1,4-disubstituted-1,2,3-triazoles under optimized reaction conditions was explored (Table 4). The reaction of different benzyl halides including electron-donating and electron-withdrawing groups with phenyl acetylene and sodium azide was explored. All corresponding triazoles were synthesized regioselectively in high yields. Electron withdrawing or electron releasing had no significant effect on the reaction time and yield of the respective product (Table 4). Moreover, reaction of various alkyl halides with phenyl acetylene and sodium azide was also studied. It was found that related products were obtained in good to high yields and in short reaction times with high regioselectivity.

A possible mechanism for this process is shown in Scheme 2. At first, Cu (II) gets partially reduced to Cu (I) state after treatment with NaN_3 and therefore is presented as Cu(II)/Cu(I) mixed valency dinuclear species. Nucleophilic attack of bnzyl azide and then phenyl acetylene provides a six-member ring which is then becomes a five-member followed by copper removal, and gives the corresponding product [11].

The catalyst recyclability was also evaluated under the optimized conditions. For this purpose, the reaction of benzyl chloride with phenyl acetylene and sodium azide was investigated. After reaction completion, the catalyst was separated and washed with hot ethanol. Then, it was dried and stored for subsequent reaction. This process was performed more than 6 times, and results showed that recycled catalyst retained its catalytic activity well and the products were obtained in high yields (Table 5). Furthermore, the leaching of the Cu into the reaction mixture using ICP-AES was investigated. It was found that the difference between the copper content of the

Table 3 Effect of CuO loading on the yield of the reaction model[a]

Entry	CuO loading	Catalyst (g)	Time (min)	Yield (%)[b]
1	5	0.02	90	Trace
2	5	0.04	90	40
3	5	0.08	90	50
4	9.4	0.02	60	70
5	9.4	0.04	12	92
6	9.4	0.08	12	92
7	15	0.02	45	70
8	15	0.04	15	91
9	15	0.08	10	92

[a]Reaction conditions: benzyl chloride (1 mmol), phenylacetylene (1 mmol), sodium azide (1.1 mmol) in water at reflux conditions.
[b]Isolated pure products

Table 4 M-CuO nanocatalyst-catalyzed regioselective synthesis of 1,4-disubstituted-1H-1,2,3-triazoles

Entry	Substrate	Time (min)	Yield (%)[a]	M.P. (°C)[b]
1	$C_6H_5CH_2Cl$	12	92	130–131
2	$3\text{-}MeC_6H_4CH_2Cl$	15	92	108–110
3	$4\text{-}MeC_6H_4CH_2Cl$	15	91	110–111
4	$4\text{-}MeOC_6H_4CH_2Cl$	15	92	140–141
5	$3\text{-}ClC_6H_4CH_2Cl$	20	91	107–109
6	$2\text{-}ClC_6H_4CH_2Cl$	22	90	88–89
7	$2,4\text{-}Cl_2C_6H_3CH_2Cl$	20	92	148–150
8	$4\text{-}NO_2C_6H_4CH_2Cl$	25	90	155–157
9	$4\text{-}BrC_6H_4CH_2Cl$	15	90	152–154
10	$MeCH_2Cl$	25	89	61–63
11	$n\text{-}C_4H_9Cl$	30	88	47–48
12	$n\text{-}C_5H_{11}Cl$	30	88	70–72
13	$C_6H_5CH_2Cl$	20	91	137–139[c]

[a]Isolated yields. [b]Products were characterized by comparison of their spectroscopic data and melting points with those reported in the literature [5, 8, 22, 27]. [c]Corresponding product was obtained from reaction of benzyl chloride, sodium azide and *p*-methoxy phenyl acetylene [8]

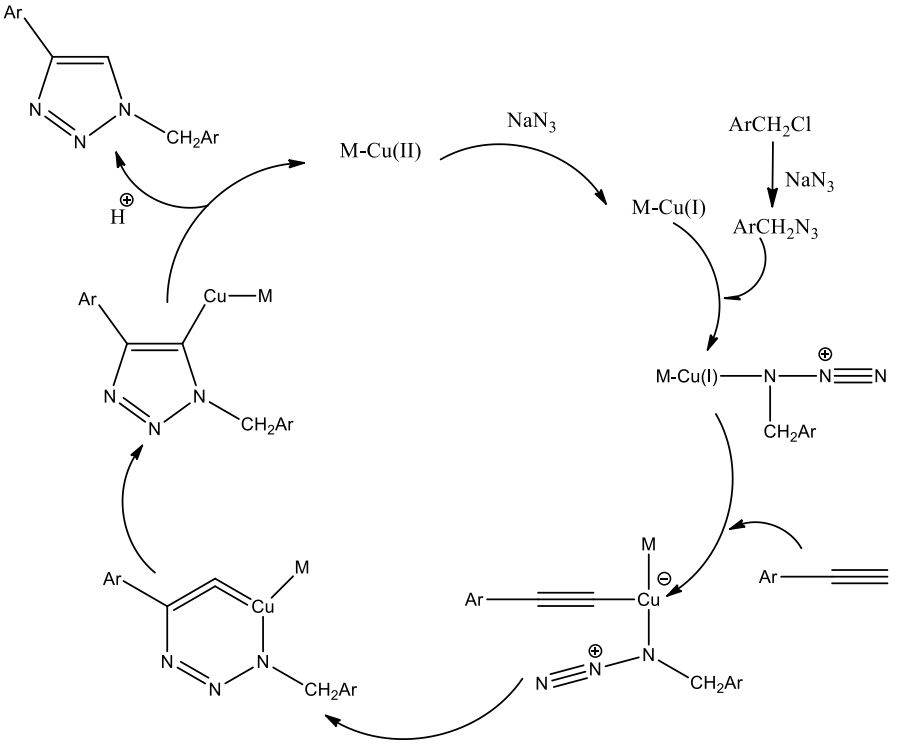

Scheme 2 Proposed synthesis of 1,4-disubstituted-1H-1,2,3-triazoles catalyzed by M-CuO nanocatalyst

Table 5 Resubility study of M-CuO nanocatalyst

Run	1	2	3	4	5	6
Time (min)	12	12	12	15	18	20
Yield (%)[a]	92	91	90	90	88	85

[a]Isolated yield

fresh catalyst and the reused catalyst (5th run) was only 3.3% which showed the low leaching amount of copper oxide catalyst into the reaction mixture.

Conclusion

In summary, we have reported the preparation, characterization and catalytic activity of M-CuO nanocatalyst as an efficient recyclable nanocatalyst for the regioselective synthesis of 1,4-disubstituted-1H-1,2,3-triazoles in water. This new nanocatalyst is easily prepared, is easy to handle and can be recovered more than 6 runs by simple filtration. Furthermore, regioselective reactions, clean procedure, simple workup, heterogeneous reaction conditions, high yields of products and short reaction times are other advantages of this method.

Acknowledgements We are thankful to the Shahrekord University for the support of this work.

References

1. S. Kantheti, R. Narayan, K.V.S.N. Raju, P.S. Sarath, R. Narayan, K.V.S.N. Raju, RSC. Adv. **5**, 3687 (2015)
2. Y. Xia, Z. Fan, J. Yao, Q. Liao, W. Li, F. Qu, L. Peng, Bioorg. Med. Chem. Lett. **16**, 2693 (2006)
3. R. Huisgen, Pure Appl. Chem. **61**, 613 (1986)
4. R. Huisgen, Angew. Chem. **75**, 604 (1963)
5. K. Gonzales-Silva, D. Rendon-Nava, A. Alvarez-Hernández, D. Mendoza-Espinosa, New J. Chem. **43**, 16538 (2019)
6. H. Naeimi, S. Dadashzadeh, M. Moradian, Res. Chem. Intermed. **41**, 2687 (2015)
7. C. Sharma, M. Kaur, A. Choudhary, S. Sharma, S. Paul, Catal. Lett. **159**, 82 (2020)
8. A. Pathigoola, R.P. Pola, K.M. Sureshan, Appl. Catal A Gen. **453**, 151 (2013)
9. V.D. da Silva, B.M. de Faria, E. Colombo, L. Ascari, G.P.A. Freitas, L.S. Flores, Y. Cordeiro, L. Romão, C.D. Buarque, Bioorg. Chem. **83**, 87 (2019)
10. M. Gholinejad, E. Oftadeh, J.M. Sansano, ChemistrySelect **4**, 3151 (2019)
11. M. Shabber, A.K. Padala, B.A. Dar, B. Singh, B. Sreedhar, R.A. Vishwakarma, S.B. Bharate, Tetrahedron **68**, 8156 (2012)
12. F. Faeghi, S. Javanshir, S. Molaei, Appl. Organomet. Chem. **3**, 11427 (2018)
13. N. Touj, I. Özdemir, S. Yasar, N. Hamdi, Inorg. Chim. Acta **467**, 21 (2017)
14. A.R. Hajipour, M. Karimzadeh, F. Fakhari, H. Karimi, Appl. Organomet. Chem. **30**, 964 (2016)
15. S. Bahadorikhalili, L. Ma'mani, H. Mahdavi, A. Shafiee, Microporous Mesoporous Mater. **262**, 207 (2018)
16. N. Touj, A. Chakchouk-Mtibaa, L. Mansour, A.H. Harrath, J.H. Al-Tamimi, I. Özdemir, L. Mellouli, S. Yaşar, N. Hamdi, J. Organomet. Chem. **853**, 49 (2017)
17. M. Kumari, Y. Jain, P. Yadav, H. Laddha, R. Gupta, Catal. Lett. **149**, 2180 (2019)
18. M. Tajbakhsh, M. Farhang, S.M. Baghbanian, R. Hosseinzadeh, M. Tajbakhsh, New J. Chem. **39**, 1827 (2015)
19. A. Keivanloo, M. Bakherad, M. Khosrojerdi, A.H. Amin, Res. Chem. Intermed. **44**, 2571 (2018)

20. A.R. Sardarian, F. Mohammadi, M. Esmaeilpour, Res. Chem. Intermed. **45**, 1437 (2019)
21. M.A. Karimi Zarchi, F. Nazem, J. Iran. Chem. Soc. **11**, 1731 (2014)
22. M. Keshavarz, R. Badri, Mol. Divers. **15**, 957 (2011)
23. A. Coelho, P. Diz, O. Caamaño, E. Sotelo, Adv. Synth. Catal. **352**, 1179 (2010)
24. U. Sirion, Y.J. Bae, B.S. Lee, D.Y. Chi, Synlett. **2008**, 2326 (2008)
25. H. Naeimi, R. Shaabani, Catal. Commun. **87**, 6 (2016)
26. B. Gerard, J. Ryan, A.B. Beeler, J.A. Porco, Tetrahedron **62**, 6405 (2006)
27. J. Albadi, A. Alihosseinzadeh, A. Mansournezhad, Synth. Commun. **45**, 877 (2015)
28. Z. Sotoudehnia, J. Albadi, A.R. Momeni, Appl. Organomet. Chem. **33**, e4625 (2019)
29. J. Albadi, A. Alihoseinzadeh, M. Jalali, M. Shahrezaei, A. Mansournezhad, Mol. Catal. **440**, 133 (2017)
30. J. Albadi, A. Alihosseinzadeh, A. Mansournezhad, Acta Chim. Slov. **62**, 617 (2015)
31. J. Albadi, A. Mansournezhad, Res. Chem. Intermed. **42**, 5739 (2016)
32. X. Wen, W. Zhang, S. Yang, Langmuir **19**, 5898 (2003)
33. N. Kanagatha, N. Sivakumar, K. Gayathri, P. Krishnan, N.G. Renganathan, S. Gunasekaran, G. Anbalagan, Proc. Indian Natl. Sci. Acad. **79**, 467 (2013)
34. E.W. Hughes, J. Am. Chem. Soc. **63**, 1737 (1941)
35. V. Vellora, T. Padil, M. Cernik, Int. J. Nanomed. **8**, 889 (2013)
36. J. Albadi, M. Jalali, A.R. Momeni, Res. Chem. Intermed. **44**, 2395 (2018)